

Strain measurement of bellows by picture processing at elevated temperature

A.Miyoshi

Technical Research Institute, Hazama-Gumi Ltd, Yono, Japan

A.Yoshioka & G.Yagawa

Department of Nuclear Engineering, University of Tokyo, Japan

1 INTRODUCTION

Strain measurement of specimens for fundamental tests of the FBR components is often carried out at an elevated temperature (Campbell 1981, Nakanishi 1985), and weldable strain gages are usually used for that purpose. These gages, however, are not necessarily appropriate for specimens with a curved surface like bellows.

The authors have developed an optical strain measurement method and a rig using the method that measures two-axial strain like a rosette gage. It can measure strain on specimens with a curved surface at an elevated temperature, although existing optical measurement methods (Yagawa 1984, Obata 1983) can only be applied to plane specimens.

2 MEASUREMENT METHOD AND RIG

The new optical strain measurement method utilizes stereoimaging in order to measure the depth of the marks painted on the specimen. Figure 1 presents a mark P on a specimen and its images Q_a and Q_b at two camera positions. In practice, the marks are made of three solid circles painted in a small region on the specimen such that the region is approximately plane. Analysis of the two images of the marks at consecutive loading stages gives the 3 dimensional location of the marks at each stage (See Fig. 2). So the method can account for tilting of the specimen surface during loading.

By comparing the 3 dimensional locations before and after deformation for each mark, displacements will be obtained. Strain is calculated by assuming a constant strain triangle element of the FEM.

The spatial coordinates (x,y,z) of a mark P are given in the following equations.

$$(1) \quad x = x' \cos \gamma - y' \sin \gamma + D_a \sin \alpha,$$

$$(2) \quad y = x' \sin \gamma + y' \cos \gamma + D_a \cos \alpha,$$

$$(3) \quad z = z',$$

$$(4) \quad x' = \frac{z'(X_a + s_a \tan \alpha')(X_b \tan \beta' + s_b)}{(X_a \tan \alpha' - s_a)(X_b - s_b \tan \beta') + (X_b \tan \beta' + s_b)(X_a + s_a \tan \alpha')},$$

$$(5) \quad y' = \frac{-l'(X_a \tan \alpha' - s_a)(X_b \tan \beta' + s_b)}{(X_a \tan \alpha' - s_a)(X_b - s_b \tan \beta') + (X_b \tan \beta' + s_b)(X_a + s_a \tan \alpha')} ,$$

(6) and $z' =$

$$\frac{Y_a l'(X_b \tan \beta' + s_b)}{\cos \alpha' \{ (X_a \tan \alpha' - s_a)(X_b - s_b \tan \beta') + (X_b \tan \beta' + s_b)(X_a + s_a \tan \alpha') \}} ,$$

where x axis is defined by the rotational axes of the camera at two camera positions (See Fig. 3), and x' axis is defined by the principal points of the lens at two camera positions. D_a and D_b is the distance between a principal point of the lens and the rotational axis of the camera, and α and β are the angles of rotational movement at camera position a and b respectively. l is the distance between the two camera positions a and b , and Y is the angle between x axis and x' axis. s_a and s_b are the distance between the principal point of the lens and the image.

The strain measurement rig shown in Fig. 4 is controlled by a personal computer (8086 CPU with 8087 co-processor) that carries out an on-line strain calculation. A solid state TV camera (or Charge Coupled Device, pixels 510H x 492V) is placed on an X-Y-rotation motion control stage (See Photo 1). The stage is driven by three stepping motors. The unit motion length in X and Y direction is 0.02 mm, and the unit rotation angle is 0.0135°. The two camera angles are 200 mm apart.

A frame of image data taken by the TV camera can be digitized and stored by a frame memory (pixels 640H x 482V, 256 gray levels) and sent to the personal computer's main memory. Both the raw picture and the processed picture can be displayed on a TV monitor.

3 PICTURE PROCESSING

The role of picture processing in this strain measurement is to find an accurate location of a mark. The procedure is divided into pre-processing and main processing to save processing time.

In the pre-processing, a rough location of a gage mark is obtained from coarsely sampled picture data (160H x 120V out of 640H x 482V). In the main processing, an accurate location of a mark is found from fine picture data within a small window (about 50 x 50 pixels) determined in the pre-processing.

The algorithm in the pre-processing is given in the following.

1. Smoothing is performed to remove fine noise.
2. Laplacian is operated to level sloped gray level while conserving the shape of the mark: If the specimen surface is curved, background gray level is uneven and marks are sometimes difficult to detect. By using Laplacian, the peaks of marks become higher compared with background.
3. The picture data is binarized.

4. Mark candidates are detected by following borders (Rosenfeld 1982) in the binarized picture. Then, real marks are distinguished from noise by using the complexity (perimeter²/area), area and aspect ratio of the mark candidates. This method makes mark recognition possible even if the picture has a lot of noise. The circumrectangular of marks is used as a window in the main processing.

In the main processing, gray scale of the smoothed picture is stretched to increase contrast. Then, a center of geometry of a mark is calculated

for a binarization threshold level. Average is taken for five different binarization levels. Resolution of mark detection by this method is about a tenth of a pixel.

4 VALIDATION TEST

In order to confirm accuracy of strain measured by picture processing, validation tests were performed both at the room temperature and at an elevated temperature.

First, tensile tests were performed on a plate and a bellows made of AISI type 316L stainless steel at the room temperature. The results of the plate test are shown in Fig. 5. Strain by picture processing is plotted against that measured by 2mm length high strain gages glued just behind the marks. The observed error was 260 to 2000 μ ($1\mu = 10^{-6}$). This was satisfactorily small compared with the estimated maximum error of 0.5 % (5000 μ).

The bellows specimen and four gage marks are presented in Fig. 6. Location A is at a crown apex. Location B is slightly deviated from the crown apex: the normal to the surface is 20° upward from the horizontal level. Location C is at a root bottom, and location D is also deviated from the root bottom: the normal is 20° upward from the horizontal level. For each mark location, three pairs of crossed high strain gages of 2mm length were glued for comparison.

Strain-load relation at location A is shown in Fig. 7. The error was 1100 to 5900 μ for axial strain and 730 to 8500 μ for hoop strain, which was larger than that for the plate. Other marks gave similar results.

Next, tensile loading tests were carried out on a plate specimen of type 316 stainless steel and a cylindrical specimen of type 304 stainless steel at 550°C by using the electro-magnetic induction heating.

On the plate specimen shown in Fig. 8, three marks were spray-painted by silver colored heat-resistant paint to assure contrast against the steel that will become brown at elevated temperatures. Optically measured strains through a Pyrex window were compared with those obtained from elongation measured by displacement transducers attached at the end of stainless steel arms welded to the plate as in Fig. 8. The lens was set 350 mm apart from the specimen, and the parallax between the two camera positions was about 33°.

Strains by optical measurement that was made three times at each strain level are plotted with those obtained from elongation of the plate against the load in Fig. 9. As seen from the figure, the error is within 2000 μ , which is the same as that for the plate at the room temperature.

The cylindrical specimen is shown in Fig. 10. Three silver-colored marks were put by using the screen printing at the location where the normal to the surface is 10° upward from the horizontal level. Steel arms similar to those for the plate were welded to measure elongation of the vertical diameter of the cylinder when loaded in tension.

On the other hand, an FEM analysis was carried out on the cylinder's 9 element quarter-symmetric model by using MARC's isoparametric curved beam element. The elongation of the diameter was used as a boundary displacement. In Fig. 11, optically measured hoop strains and those by the FEM are plotted against the elongation. The error between the analysis and measurement was within 2400 μ , which is nearly the same as those of other tests except the bellows test. It is assumed that a reason for the larger errors in the bellows test was because marks were glossy.

5 DISCUSSION

Knowledge gained in the tests are summarized below.

1. The color of marks has to be chosen according to the color of specimens so that good contrast is assured.
2. Generally speaking, direct lighting is undesirable because it reveals scratches on the specimen thus increase noise in the image, while indirect lighting increase contrast.
3. Error becomes smaller as focusing becomes better.
4. A single measurement takes about fifty seconds. This has been greatly reduced by algorithm refinement, reduction of keyboard typing and picture processing performed simultaneously with camera movement. Also, decision of binarization threshold level in the pre-processing was automated.
5. The strain measurement method proposed here was found essentially applicable to a specimen that has curvature both in the axial and circumferential direction such as bellows and spheres. However, lighting condition varies as load increases because the slope of specimens' surface varies as it deforms. So, a great care must be paid to lighting.
6. Shape recognition used to distinguish marks from noise has greatly reduced chances of false mark recognition.
7. There were no essential problems with regard to measurement at elevated temperature so long as induction heating was used although image blurring by convection of air, optical influence due to the presence of the Pyrex window and overheating of the camera had been expected.

6 SUMMARY

1. An optical strain measurement system that can be used to specimens with a curved surface was developed, and its practicability in large strain measurement was confirmed at elevated temperatures.
 2. Several improvements were made on picture processing algorithm to achieve a quicker measurement and an automated mark detection.
 3. Tests were performed on a plate and a cylindrical specimen at 550°C. Errors for the plate were within 2000 μ , and 2400 μ for the cylinder. They were comparable with those for the plate at the room temperature.
- The present work is a result of the Joint Research Program between University of Tokyo and the Hazama-Gumi, Ltd..

REFERENCES

- Campbell, R.D. & T.R.Kipp. 1981. Accelerated testing of flexible piping joints operating at creep temperature. ASME PVP 51:75-89.
- Nakanishi, S. et al. 1985. Thermal transient test facility for structures. Trans. Int. Conf. Struct. Mech. in React. Technol. 8:E2/1.
- Obata, M. et al. 1983. Fine-grid method for large-strain analysis near a notch tip. Exp. Mech. 23:146-151.
- Rosenfeld, A. & A.C.Kak. 1982. Digital Picture Processing. Orlando: Academic Press.
- Yagawa, G. & S.Matsuura. 1984. Strain distribution around a crack tip in high temperature environment using picture processing. Nucl. Eng. Des. 83:259-265.

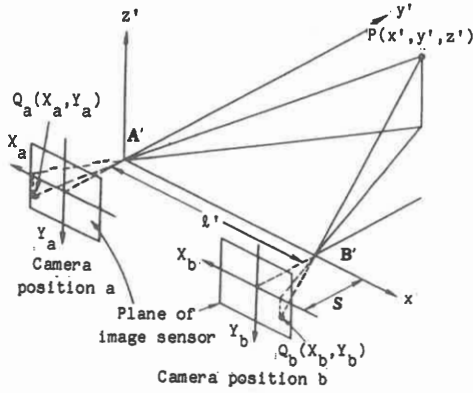


Fig. 1 Stereoviewing

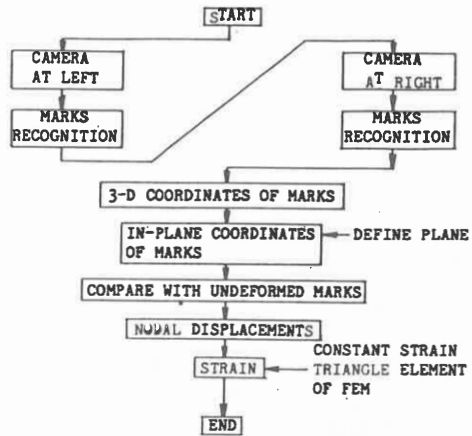


Fig. 2 Strain measurement flow

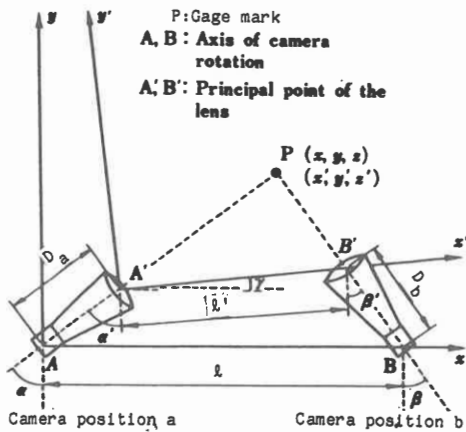


Fig. 3 Transformation of coordinate systems based on camera rotation

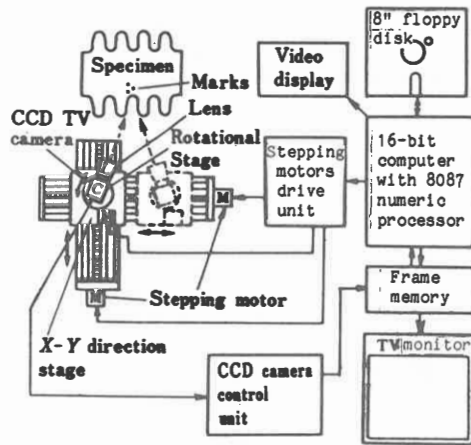


Fig. 4 Block diagram of strain measurement system

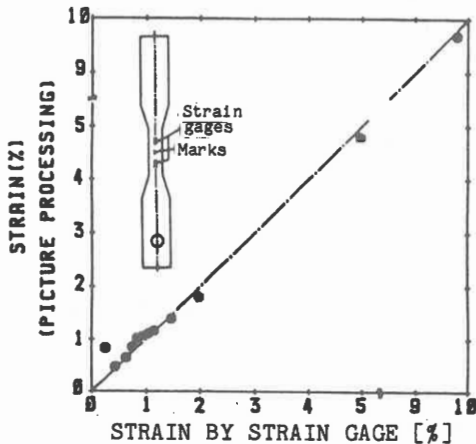


Fig. 5 Comparison of strains measured by strain gage and picture processing (Plate, ROOM temperature)

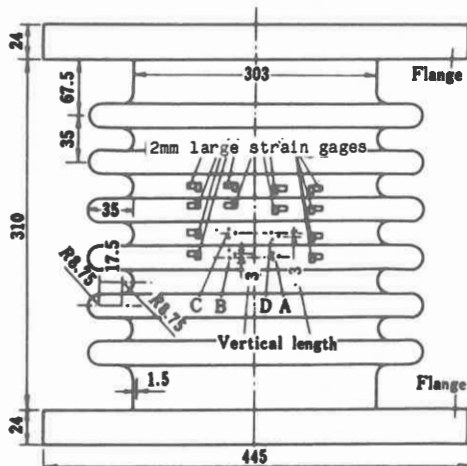


Fig. 6 Bellows specimen, location of marks and strain gages

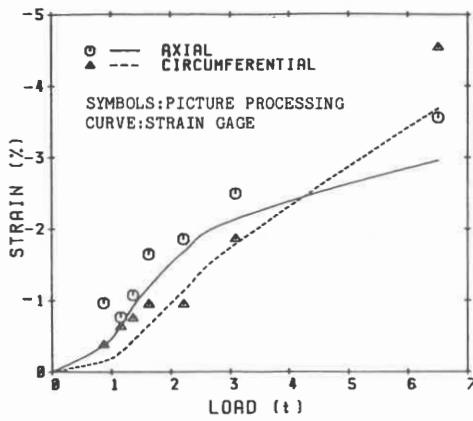


Fig. 7 Comparison of strains measured by strain gage and picture processing (Bellows, room temperature)

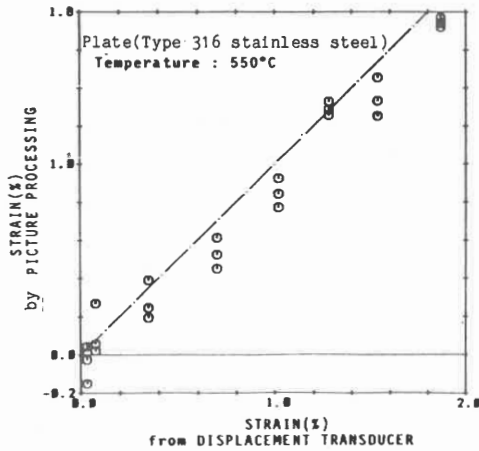


Fig. 9 Comparison of strain obtained from elongation with that by picture processing (Plate, at 550°C)

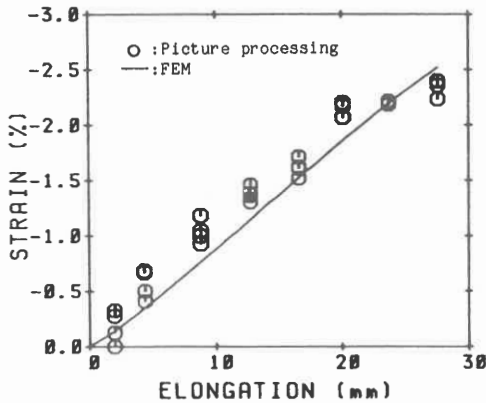


Fig. 11 Comparison of strains by FEM analysis and picture processing (Cylinder, at 550°C)

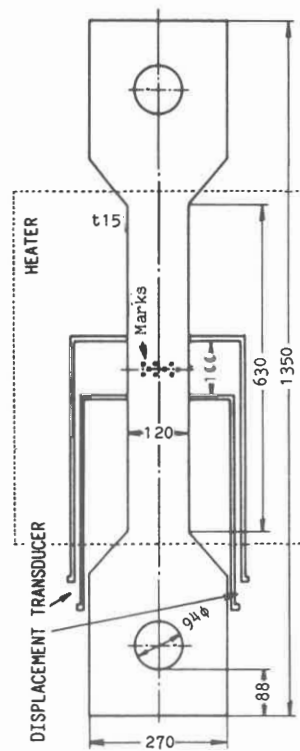


Fig. 8 Plate specimen for test at 550°C

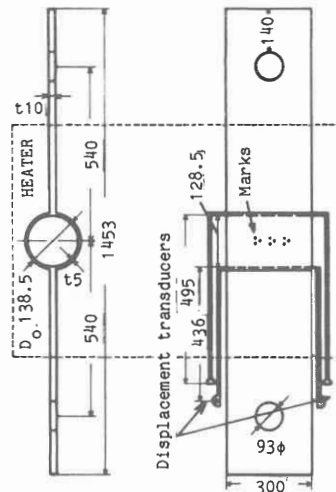


Fig. 10 Cylindrical specimen and mark locations